

Tunable Photoinduced Carrier Transport of a Black Phosphorus Transistor with Extended Stability Using a Light-Sensitized Encapsulated Layer

Po-Hsun Ho,^{†,#} Min-Ken Li,^{†,#} Raman Sankar,[‡] Fu-Yu Shih,^{§,⊥} Shao-Sian Li,[†] Yih-Ren Chang,[†] Wei-Hua Wang,[⊥] Fang-Cheng Chou,^{‡,||} and Chun-Wei Chen^{*,†,||}

[†]Department of Materials Science and Engineering, [‡]Center for Condensed Matter Sciences, and [§]Department of Physics, National Taiwan University, Taipei 10617, Taiwan

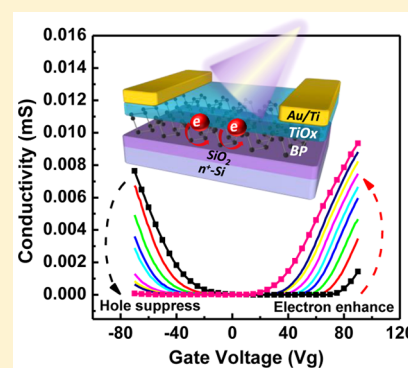
[⊥]Institute of Atomic and Molecular Sciences, Academia Sinica, Taipei, 10617, Taiwan

^{||}Taiwan Consortium of Emergent Crystalline Materials (TCECM), Ministry of Science and Technology, Taipei, Taiwan

Supporting Information

ABSTRACT: In this article, we propose a novel approach to demonstrate tunable photoinduced carrier transport of a few-layered black phosphorus (BP) field-effect transistor (FET) with extended air stability using a “light-sensitized ultrathin encapsulated layer”. Titanium suboxide (TiO_x) ultrathin film (approximately 3 nm), which is an amorphous phase of crystalline TiO₂ and can be solution processed, simultaneously exhibits the unique dual functions of passivation and photoinduced doping on a BP FET. The photoinduced electron transfer at TiO_x/BP interfaces provides tunable n-type doping on BP through light illumination. Accordingly, the intrinsic hole-dominated transport of BP can be gradually tuned to the electron-dominated transport at a TiO_x/BP FET using light modulation, with enhanced electron mobility and extended air stability of the device. The novel device structure consisting of a light-sensitized encapsulated layer with controllable and reversible doping through light illumination on BP exhibits great potential for the future development of stable BP-based semiconductor logic devices or optoelectronic devices.

KEYWORDS: black phosphorus, field-effect transistor, n-type, stability, photodoping



Although graphene exhibits excellent carrier transport because of unique two-dimensional (2D) energy dispersion, the absence of an intrinsic band gap of graphene largely limits its application in semiconductor logic devices. The 2D-layered materials of transition-metal dichalcogenides (TMDs) with inherent band gaps such as MoS₂ and WS₂ have recently demonstrated great potential as the building blocks for next-generation semiconductor logic devices by enabling ultrathin high-quality semiconducting channels.^{1,2} Another emerging 2D material is black phosphorus (BP)—or phosphorene—which consists of a one-atom-thick sheet of phosphorus atoms, with each atom forming the puckered orthorhombic structure, and is the second known 2D atomic crystal other than graphene that is formed by a single chemical element.^{3,4} Ultrathin few-layer or monolayer BP flakes have been exfoliated successfully from a bulk BP crystal because of weak interlayer van der Waals interactions.³ Unlike semiconducting TMDs, BP has a direct band gap for all numbers of layers, from 1.2 eV for the monolayer to 0.3 eV for a bulk BP.⁵ Ultrathin few-layer BP field-effect transistors (FETs) exhibiting excellent semiconductor transport behavior with remarkably high hole mobilities up to 1000 cm² V⁻¹ s⁻¹ and an on–off ratio in the range 10²–10⁵ at room temperature have been

demonstrated recently,³ making them promising for semiconductor logic device applications. However, critical challenges remain for BP to be realized in the practical application of 2D electronic devices. First, the low chemical stability of BP has been widely reported, which undergoes fast degradation after exposure to ambient air, because oxygen and moisture can cause severe compositional and physical changes in the material.⁶ Several passivation techniques such as using the atomic layer deposition (ALD) of AlO_x overlayers⁷ or the transfer of atomically thin graphene and hexagonal boron nitride^{8,9} as capped layers have been developed to effectively prevent deterioration in BP devices. In addition, the ambipolar characteristics of BP FETs typically show strong asymmetric electron and hole transport behaviors, with an electron mobility in order of magnitudes lower than its hole mobility,^{3,7,9} so that the task of obtaining a high-performance n-type BP FET is generally more challenging than for its p-type counterpart.¹⁰ Therefore, the solutions of these two critical issues in the search for a stable and high-performance n-type BP FET will have a

Received: March 17, 2016

Published: May 23, 2016

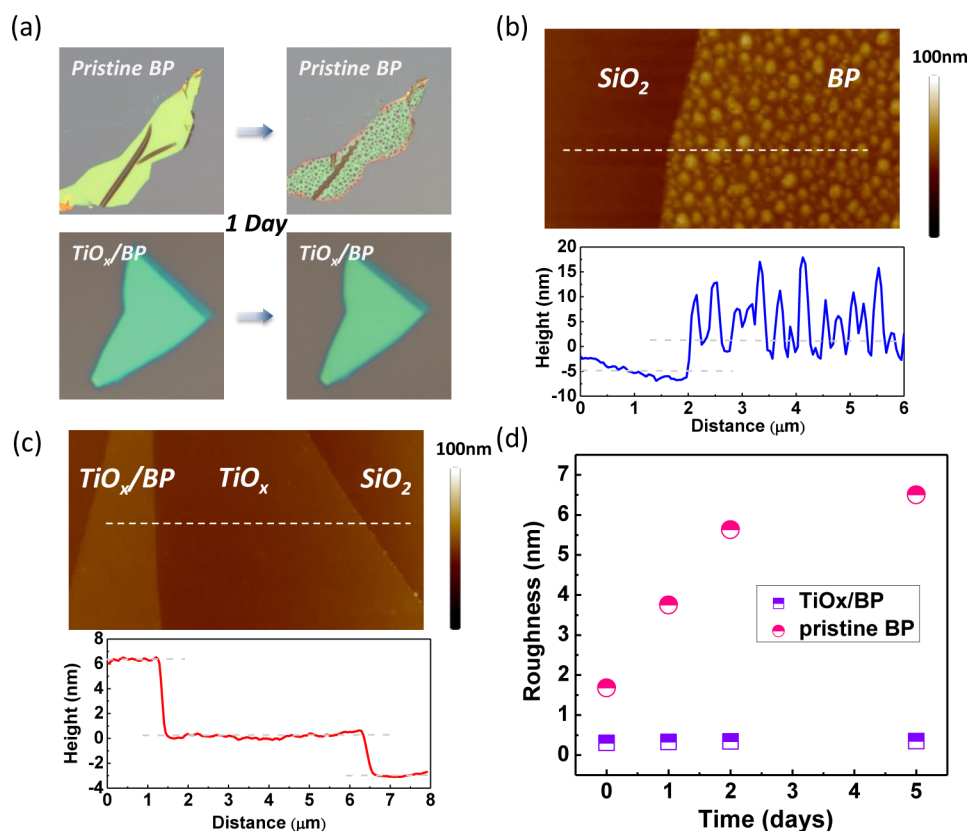


Figure 1. (a) Optical image of few-layer BP without/with coating the TiO_x film before and after aging for 1 day. AFM images and line profiles of (b) the pristine BP and (c) TiO_x/BP samples after aging for 1 day. (d) Time-dependent evolution of surface roughness of BP with and without coating with the TiO_x film.

great impact in this emerging field for the future development of BP-based complementary logic devices.

In 2D atomic-layered materials, because the entire surface is exposed to its surroundings, the tunable electrical properties of both n-type and p-type transport are attainable through the chemical doping of either substitutional doping¹¹ or surface charge-transfer doping.¹² Chemical doping based on surface charge transfer by depositing a thin cesium carbonate (Cs₂CO₃) layer has recently been used to modulate the electron transport behavior of a few-layered BP FET with a substantial increase in electron mobility by filling high concentrations of electron traps of undoped BP.¹² The doping concentrations of chemical doping are typically controlled through the thickness or concentration of dopants.^{11,12} Another promising approach to modulating the electrical properties of graphene^{13,14} or TMD-based^{15,16} transistors by using optical excitation has been recently demonstrated. The unique advantage of using photoinduced doping on modulating carrier transport behaviors is that this technique is more controllable and reversible than is chemical doping,^{13–16} in which photogenerated charges from a light-absorbing material can be transferred to the surface of 2D atomic layer materials, resulting in controllable p- or n-doping processes through light illumination. This work demonstrates a novel approach for fabricating a tunable photoinduced carrier transport of a few-layer BP FET, with carrier concentrations and carrier transport types to be controlled through light modulation. The photoactive layer of an ultrathin titanium suboxide (TiO_x) film (approximately 3 nm), which is an amorphous phase of crystalline TiO₂ and can be solution processed,¹⁷ simulta-

neously exhibits the unique dual functions of passivation and photoinduced n-type doping on a BP FET, as a result of trap-state-mediated photoinduced charge transfer at the BP/TiO_x interface. Through light modulation on the BP FET using an encapsulated photodoping layer of a TiO_x ultrathin film, the intrinsic hole-dominated transport of a BP FET can be tuned gradually to an electron-dominated transport, accompanied by enhanced electron mobility and extended air stability of the device. To our knowledge, this is the first report of modulating carrier transport behavior of a black phosphorus FET through photoinduced doping.

RESULTS AND DISCUSSION

The bulk BP single crystals were grown via a SnI₄ chemical vapor transport (CVT) method in our lab, where a high-quality BP single crystal with a large size of more than 0.7 cm was obtained (see Supporting Information). The detailed synthesis processes of growing single-crystal BP are described in the Supporting Information. Few-layered BP was exfoliated from a bulk BP crystal by using a conventional Scotch tape method before it was transferred to a SiO₂/Si substrate. Because of the intrinsically unstable properties of few-layered BP, the surface of as-exfoliated BP was degraded quickly through oxidation in ambient air. The optical images in the top panel of Figure 1a display the evolution of the as-exfoliated few-layered BP on silica after exposure to the ambient atmosphere (25 °C, 50% humidity) for 1 day. The initial uniform optical contrast of the few-layered BP sample indicated that the as-cleaved surface was smooth because of its layer structure. However, after exposure to the ambient atmosphere for 1 day, the BP optical image

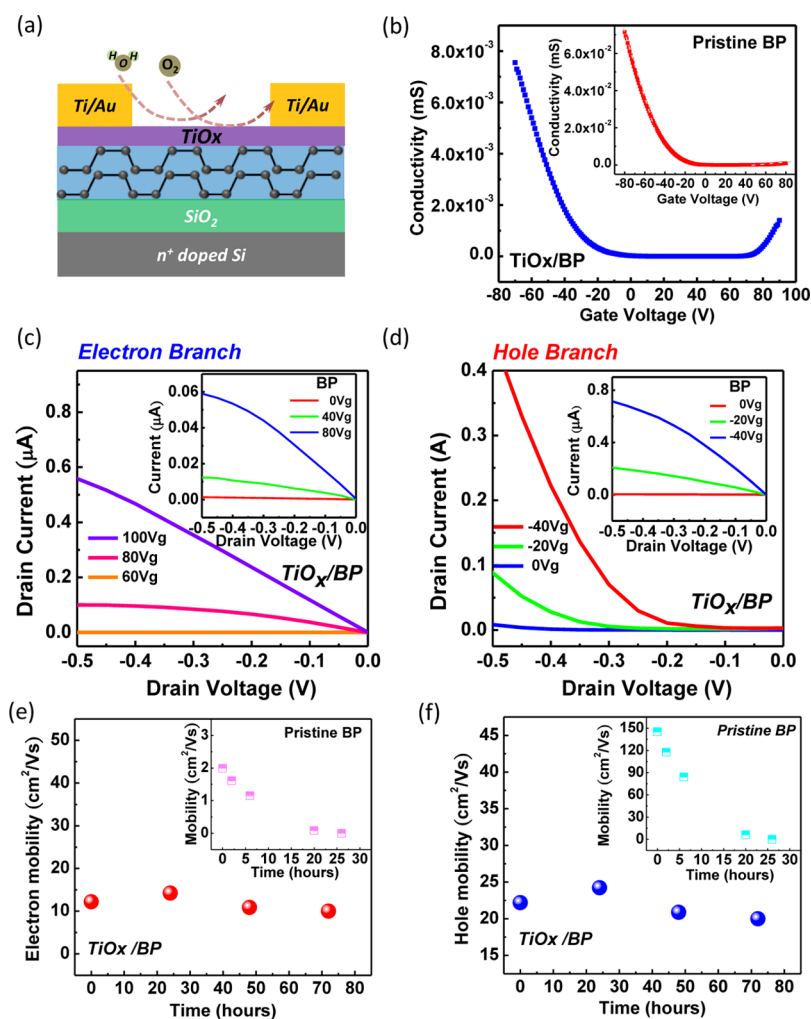


Figure 2. (a) Schematic representation of a precoated TiO_x/BP FET. (b) Gate-dependent conductivity of the TiO_x/BP FET and the pristine BP FET (inset). (c and d) Transport characteristics of source–drain voltage versus current of the electron and hole branches, respectively. (e and f) Stability test of the TiO_x/BP and pristine BP (inset) transistors.

became nonuniformly gray, and many particles formed on the surface (Figure 1a, top right). The corresponding surface morphology of BP was further analyzed using atomic force microscopy (AFM), as shown in Figure 1b, where many oxidized particles with sizes of 20–200 nm in width and 5–30 nm in height can be clearly observed. In this work, a sol–gel TiO_x thin film was used as an encapsulated layer by spin coating to protect the intrinsic few-layered BP from degradation. A detailed synthesis method of a TiO_x thin film is described in the Supporting Information. The amorphous TiO_x thin film, with a large band gap of >3 eV (Supporting Information), has been widely used as an effective encapsulated layer¹⁸ or an electron-transporting modified layer^{19,20} for enhancing the efficiencies of polymer photovoltaics. Recently, it was also found to act as an efficient electron-donating agent when fabricating stable n-type graphene transistors because of its inherent oxygen vacancies.¹⁷ Compared with the pristine unprotected BP, the uniform optical contrast of TiO_x/BP can still be maintained without any noticeable surface changes after exposure in air for 1 day, as shown in the bottom panel of Figure 1a. The corresponding AFM image of the TiO_x/BP sample was further analyzed, as shown in Figure 1c, where three distinct regions of TiO_x/BP , TiO_x , and SiO_2 can be clearly resolved, which are subject to the profiles of BP encapsulated with a TiO_x thin film (TiO_x/BP),

the TiO_x thin film on the surface of the SiO_2 substrate (TiO_x), and the pristine SiO_2/Si substrate (SiO_2), respectively. An ultrathin TiO_x film with a thickness of approximately 3 nm can be uniformly deposited through spin coating. A considerably smooth surface can be retained in the TiO_x/BP sample without the formation of any oxidized particles after exposure in ambient air for 1 day. Figure 1d shows the evolution of the average roughness of the pristine BP and TiO_x/BP samples after exposure in air for several days. The BP encapsulated with a TiO_x thin film exhibited good air stability with low surface roughness (0.35 ± 0.02 nm) compared with the pristine BP sample, the roughness (6.50 ± 0.51 nm) of which increased dramatically after exposure in air for 5 days, implying that the TiO_x ultrathin film could act as an effective encapsulated layer for BP. In contrast to the reported passivation techniques such as the ALD of overlayers⁷ or the transfer of atomically thin graphene and hexagonal boron nitride as capped layers,^{8,9} the simple solution-processable TiO_x thin film has the unique advantage of requiring less complicated procedures in the fabrication of large-area electronic devices.

To obtain a high-performance BP FET, it is critical to protect the BP surface from oxidation during fabrication processes, in particular for an n-type device. Özyilmaz et al. recently demonstrated a substantially improved n-type charge transport

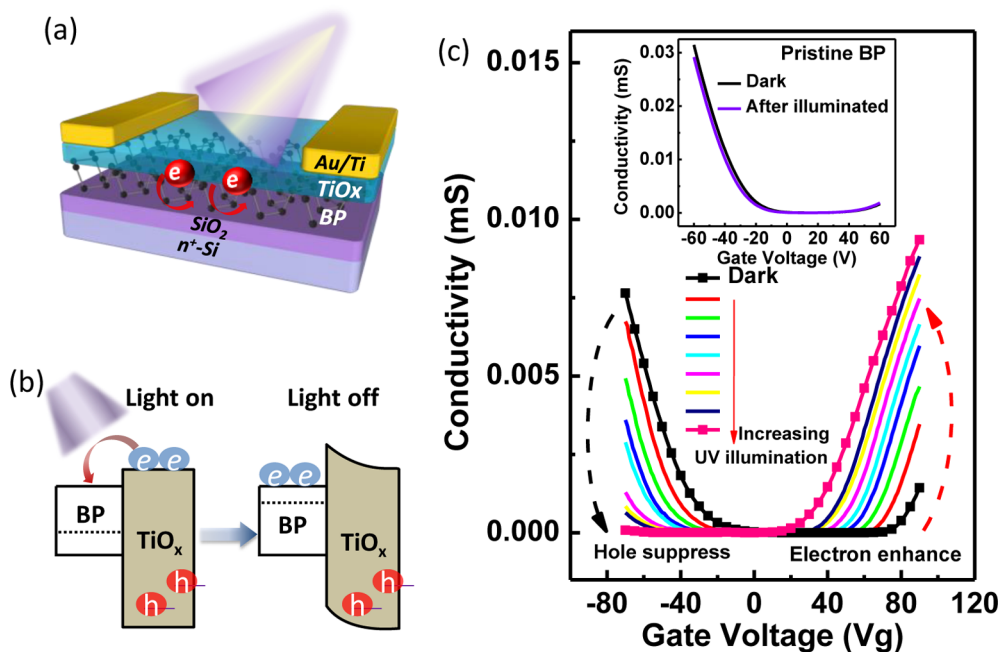


Figure 3. (a) Schematic representation of a BP/ TiO_x transistor under illumination ($\lambda = 365$ nm, power = $3.5 \times 10^{-4} \mu W/\mu m^2$). (b) Mechanism of photoinduced charge transfer at the TiO_x /BP interface. (c) Evolution of conductivity versus gate-voltage curves for the TiO_x /BP FET with increased irradiation time. The inset is the one for a pristine BP under the same illumination condition.

of a BP FET with passivation by atomically thin graphene or BN layers using the mechanical exfoliation technique in an inert atmosphere, without any prior exposure to air.⁹ Here, we propose a device structure as shown in Figure 2a where an ultrathin TiO_x film with a thickness of 3 nm was immediately deposited on the surface of the exfoliated BP sample by a spin-coating process, followed by the deposition of the source and drain electrodes on top of a precoated TiO_x /BP heterostructure. The precoated ultrathin TiO_x film may protect the BP film underneath from degradation during the fabrication of contact electrodes. Another function for the ultrathin TiO_x film in this device structure is that it can also act as an electrode modifier to enhance the electron injection efficiency as described in the following section. Figure 2b shows the gate-dependent current characteristic of the TiO_x /BP FET. For comparison, the transport behavior of the pristine unprotected BP FET is also shown in the inset. First, the appearance of a notable threshold of an electron branch in the positive bias region of the TiO_x /BP FET indicates considerable improvements in the n-type transport behavior compared with that in the pristine BP FET. The field-effect mobilities of this device (a two-terminal device) were further calculated by eq 1:

$$\mu_{FE} = \frac{L}{W} \frac{1}{C_G} \frac{dG}{dV_G} \quad (1)$$

where C_G represents the back-gate capacitance and L , W , and G are the length, width, and sheet conductance of the channel, respectively. The pristine BP exhibited asymmetric transport behavior with a predominant p-type carrier transport, with hole and electron mobilities of 145 and $2 \text{ cm}^2 \text{ V}^{-1} \text{ s}^{-1}$, respectively. These values are consistent with previously reported data on pristine BP FETs with a similar thickness.^{8,12} The predominant p-type transport of a pristine BP is mainly caused by oxidized species on the unprotected BP surface, which may act as effective electron traps in the conducting channel.⁹ For the TiO_x /BP FET, because the number of electron traps in the

conducting channel of BP is largely reduced due to the deposition of the TiO_x encapsulated layer to prevent the BP surface from oxidizing, the electron current is enhanced and the electron mobility of the TiO_x /BP FET also increases 6-fold by up to $12 \text{ cm}^2 \text{ V}^{-1} \text{ s}^{-1}$, compared to those of the pristine BP sample. Recently, Lee et al. demonstrated that the electron mobility of an n-type BP FET can be largely improved through contact-metal engineering by altering the transporting barriers of electrons and holes, where n-type contact resistance was improved while retaining suppressed hole transport.¹⁰ The thin TiO_x film, which has been widely used in organic solar cells as an effective electrode-modified layer for enhancing electron injection and hole-blocking,^{19–21} may also act as an electrode modifier for improving electron transport due to its intrinsic oxygen vacancies.^{20,22,23} The corresponding energy levels of the TiO_x thin film with respect to those of BP²⁴ and Ti/Au²⁵ electrodes are shown in the Supporting Information. A large energy difference in the valence band (VB) edges between the Ti/Au metal electrode and the thin TiO_x layer may lower the hole injection efficiency, which accounts for the suppressed hole current and the reduced effective hole mobility ($\sim 24 \text{ cm}^2 \text{ V}^{-1} \text{ s}^{-1}$) of the TiO_x /BP FET due to the hole-blocking nature of TiO_x . Accordingly, the insertion of an ultrathin TiO_x film between the BP conduction channel and metal contact electrodes not only prevents the BP surface from oxidizing but also leads to modification in the injection barriers of carriers for the TiO_x /BP FET. Figure 2c exhibits the enhanced source–drain current of the electron branch with the insertion of the TiO_x ultrathin layer at the TiO_x /BP FET, whereas Figure 2d shows the decreased hole current at the TiO_x /BP FET compared to those in the pristine BP counterpart, mainly attributed to the intrinsic nature of enhancing electron injection and suppressing hole transport of the TiO_x layer.^{19–21} The TiO_x /BP FET exhibited good stability with nearly unchanged electron and hole mobilities after exposure for 72 h to ambient air (Figure 2e and f). By contrast, the carrier mobilities of the

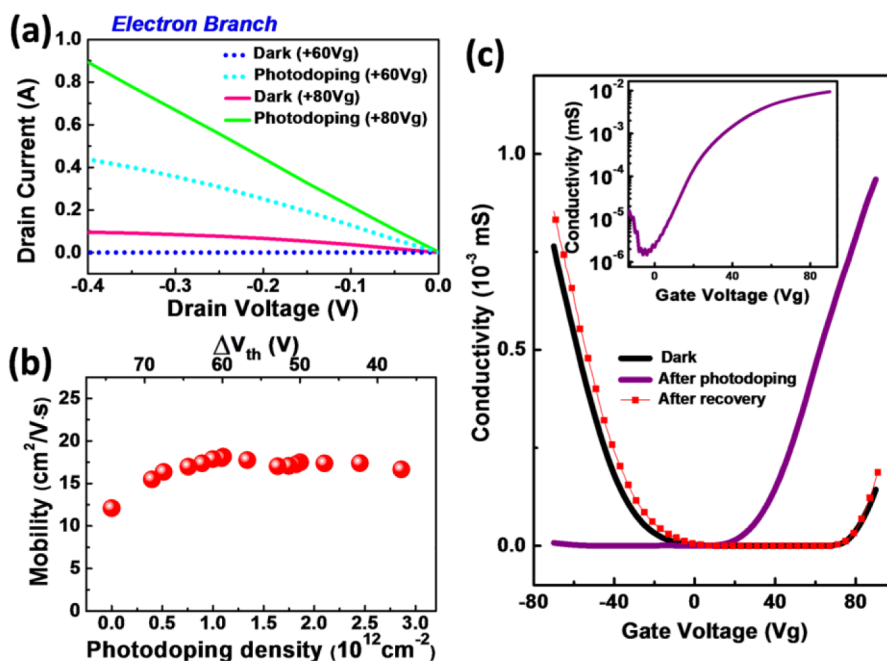


Figure 4. (a) Source–drain I – V characteristic (electron branch) of the TiO_x/BP FET before and after photoinduced doping under gate voltages of 60 and 80 V. (b) Evolution of electron mobility versus photoinduced doping density and the shift of threshold voltage ΔV_{th} for a TiO_x/BP FET. (c) Recovery process of photoinduced doping by applying a positive bias. Log-scale curve of the device after photodoping was given in the inset.

unprotected pristine BP FET degraded dramatically (the insets of Figure 2e and f). Because the main purpose of this work is to demonstrate tunable photoinduced n-type doping on a TiO_x/BP FET, the enhanced electron current and mobility of the TiO_x/BP FET with extended stability after the insertion of the ultrathin TiO_x layer are more crucial, although the hole current and mobility of the device are inevitably suppressed due to the hole-blocking effect of the thin TiO_x layer. It is worth noting that we also fabricated a postcoated TiO_x/BP FET by depositing the TiO_x film after the source and drain electrodes were deposited for the purpose of comparison. However, oxidized particles were still formed on the surface of BP during our processes of fabricating the metal electrodes so that the postcoated TiO_x/BP FET does not have a comparable device performance to the precoated TiO_x/BP counterpart (see the Supporting Information). Therefore, the deposition of a precoated TiO_x thin film to protect the BP conduction channel before the fabrication of metal electrodes as shown in Figure 2a is thus essential to be compatible with our device fabrication procedures to obtain an enhanced n-type transport of the TiO_x/BP device with extended stability.

Next, photoinduced n-type doping by modulating electron transport behavior of the TiO_x/BP FET through light illumination was demonstrated. Photoinduced doping caused by light–matter interaction at graphene– or TMD–heterostructure interfaces has recently exhibited unique physical phenomena^{14–16} and device functionality,^{13,26} where photo-generated charges from a light-absorbing material are transferred to these 2D materials, resulting in the modulation of the electronic properties of the device through light illumination. The TiO_x thin film, which has a large energy gap of >3 eV, was recently used as an efficient photoinduced electron-donating agent to graphene due to trap-state-mediated photoinduced charge transfer.¹³ Here, we used a 365 nm light-emitting diode (LED) source for exciting the photocarriers of the ultrathin TiO_x film to modulate the transport behavior of a TiO_x/BP

FET (Figure 3a). Photoexcited electron–hole pairs are generated and separated at the TiO_x/BP interfaces, as the incident photon energies are larger than the band gap of TiO_x . The nonstoichiometric TiO_x thin film consists of a large number of oxygen vacancies that typically act as effective hole-trapping centers in the gap states.^{13,20} Under light illumination, the holes are trapped in the gap states, whereas electrons in the conduction band (CB) of the TiO_x film are free to move and are thus transferred to BP, according to the band alignment as shown schematically in Figure 3b. Because of the trapped holes in the TiO_x layer as the TiO_x/BP device is under photoexcitation, the barrier height between the Fermi level of BP and the conduction band minimum (CBM) of TiO_x prevents the electrons in BP from being transferred back to TiO_x (Figure 3b, right). As the UV light is switched off, a nearly unchanged gate-dependent current–voltage characteristic curve was observed as a result of trap-state-mediated photoinduced charge transfer at the BP/ TiO_x interface. Therefore, photoinduced electron doping for a TiO_x/BP FET with a controllable doping concentration can be achieved by carefully adjusting the illumination intensity and time (dose = power \times time). Figure 3c shows the evolution of the gate-dependent conductivity curves of the TiO_x/BP FET in the dark and under different doses of UV light illumination. The power intensity was kept at a low power of $3.5 \times 10^{-4} \mu\text{W}/\mu\text{m}^2$ with a gradual increase at the irradiation time up to 1500 s. The initial transfer characteristic curve (solid black-dotted line) of the TiO_x/BP FET before light illumination exhibited typical hole-dominated transport behavior. With the gradual increase of the illuminated time of the incident light, an intriguing evolution of the gate-dependent conductivity curves of the TiO_x/BP FET was observed. The hole current at the negative sweeping voltage direction is gradually suppressed, accompanied by an increased threshold voltage as the incident photon dose is increased (solid line). By contrast, the current at the electron branch (the positive voltage direction) is gradually enhanced, accompanied

by a decreased threshold voltage. These processes reach saturation as the trapped states at TiO_x are completely filled (solid pink-dotted line), where the device exhibits an electron-dominated n-type transport behavior. The corresponding photoinduced n-type doping concentration (illuminated by $3.5 \times 10^{-4} \mu\text{W}/\mu\text{m}^2$, 1500 s) can be estimated as high as $3 \times 10^{12} \text{ cm}^{-2}$ according to $\Delta n = \alpha \times \Delta V_{\text{th}}$, where α is the calculated capacitance values at zero gate bias and ΔV_{th} is the shift of the threshold voltage. The ultrathin TiO_x film not only acts as an encapsulated layer to prevent the BP surface from oxidizing but also acts as a light-sensitized photodoping layer. Due to the intrinsic nature of enhancing electron injection or hole-blocking of the ultrathin TiO_x film, the photogenerated electrons are able to transfer to the conduction channel of BP and inject into the collecting electrodes, whereas holes are largely blocked, resulting in enhanced electron current and suppressed hole current of the device. Accordingly, tunable photoinduced n-type transport of a BP FET with extended stability can be achieved using the light-sensitized encapsulated ultrathin TiO_x layer. For comparison, we also fabricated a pristine BP FET without including the TiO_x thin film to measure the response of the electrical transport behavior under the same illumination condition ($3.5 \times 10^{-4} \mu\text{W}/\mu\text{m}^2$, 1500 s), where no obvious change after a long-term illumination has been observed (inset of Figure 3c).

Figure 4a shows the source–drain current versus the voltage characteristics of a TiO_x/BP FET under gate voltages of 60 and 80 V before and after light illumination, where the current at the electron branch increased under light illumination. The enhanced electron concentrations resulting from photoinduced charge transfer at TiO_x/BP interfaces suggests that the carrier transport behavior of a BP device can be controlled and tuned through light modulation. Figure 4b shows the relationship between the electron mobility and photoinduced doping concentration Δn and the shift of the threshold voltage ΔV_{th} . The TiO_x/BP FET exhibited improved electron mobilities of ~ 15 to $17 \text{ cm}^2 \text{ V}^{-1} \text{ s}^{-1}$ with various photoinduced doping concentrations up to $3 \times 10^{12} \text{ cm}^{-2}$. Typically, increased carrier concentrations may result in degraded carrier mobility because of enhanced scattering.²⁷ The TiO_x/BP FET preserves nearly constant electron mobility as the photoinduced doping concentration is increased without increasing Coulomb scattering from space charges. The result is the typical signature of defect-state-mediated photoinduced charge transfer as reported at a graphene/h-BN heterostructure,²⁸ where the dopants are separated from the conducting channel arising from defect states in the bulk photoactive material, similar to the conventional modulation doping in the high-electron-mobility-transistor (HEMT) technique.²⁹ The inset logarithmic plot of Figure 4c shows the $I_{\text{on}}/I_{\text{off}}$ ratio of the TiO_x/BP FET to be $\sim 10^4$ under photoinduced doping. As mentioned above, a nearly unchanged gate-dependent n-type transport characteristic curve of the TiO_x/BP FET was observed as the illuminated light was switched off (purple curve of Figure 4c). The recovery process of the TiO_x/BP FET can be achieved by applying an electric bias. The original hole-dominated transfer characteristic curve of the device before light illumination (black curve of Figure 4c) can be recovered once a positive electric bias (+100 V) is applied to the back gate of the device (red-dotted curves of Figure 4c), where electrons at the BP FET were injected back into the conduction band of TiO_x , followed by recombination with trapped holes in the gap states of TiO_x .

CONCLUSION

In summary, tunable photoinduced carrier transport of a few-layered BP FET with extended stability using a light-sensitized ultrathin encapsulated layer was demonstrated. The insertion of a solution-processable ultrathin TiO_x film between BP and contact electrodes not only protects the BP surface from oxidation but also acts as an efficient photoactive electron-donating agent. By controlling the dose of UV illumination, the initial hole-dominated transport of a TiO_x/BP FET can be gradually tuned into an electron-dominant transport, accompanied by enhanced electron mobility and extended air stability. Because the carrier transport types of the TiO_x/BP device can be controlled through light illumination, an interesting concept of a proposed device structure with light illumination on a selective area to create a BP p–n junction could be feasible, as shown in the Supporting Information, which may facilitate the future development of BP-based semiconductor logic devices or optoelectronic devices such as detectors or sensors.

ASSOCIATED CONTENT

Supporting Information

The Supporting Information is available free of charge on the ACS Publications website at DOI: 10.1021/acsp Photonics.6b00192.

Materials synthesis and characterization; details of device fabrication and measurement (PDF)

AUTHOR INFORMATION

Corresponding Author

*E-mail (C.-W. Chen): chunwei@ntu.edu.tw.

Author Contributions

#P.-H. Ho and M.-K. Li contributed equally.

Notes

The authors declare no competing financial interest.

ACKNOWLEDGMENTS

This work is supported by the Minister of Science and Technology (MOST), Taiwan (Project Nos. 103-2119-M-002-021-MY3 and 102-2119-M-002-005), and Taiwan Consortium of Emergent Crystalline Materials (TCECM).

REFERENCES

- (1) Radisavljevic, B.; Whitwick, M. B.; Kis, A. Integrated Circuits and Logic Operations Based on Single-Layer MoS₂. *ACS Nano* **2011**, *5*, 9934–9938.
- (2) Tosun, M.; Chuang, S.; Fang, H.; Sachid, A. B.; Hettick, M.; Lin, Y.; Zeng, Y.; Javey, A. High-Gain Inverters Based on WSe₂ Complementary Field-Effect Transistors. *ACS Nano* **2014**, *8*, 4948–4953.
- (3) Li, L.; Yu, Y.; Ye, G. J.; Ge, Q.; Ou, X.; Wu, H.; Feng, D.; Chen, X. H.; Zhang, Y. Black phosphorus field-effect transistors. *Nat. Nanotechnol.* **2014**, *9*, 372–377.
- (4) Brown, A.; Rundqvist, S. Refinement of the crystal structure of black phosphorus. *Acta Crystallogr.* **1965**, *19*, 684–685.
- (5) Buscema, M.; Groenendijk, D. J.; Blanter, S. I.; Steele, G. A.; van der Zant, H. S. J.; Castellanos-Gomez, A. Fast and Broadband Photoresponse of Few-Layer Black Phosphorus Field-Effect Transistors. *Nano Lett.* **2014**, *14*, 3347–3352.
- (6) Castellanos-Gomez, A.; Vicarelli, L.; Prada, E.; Island, J. O.; Narasimha-Acharya, K.; Blanter, S. I.; Groenendijk, D. J.; Buscema, M.; Steele, G. A.; Alvarez, J. Isolation and characterization of few-layer black phosphorus. *2D Mater.* **2014**, *1*, 025001.

- (7) Wood, J. D.; Wells, S. A.; Jariwala, D.; Chen, K.-S.; Cho, E.; Sangwan, V. K.; Liu, X.; Lauhon, L. J.; Marks, T. J.; Hersam, M. C. Effective passivation of exfoliated black phosphorus transistors against ambient degradation. *Nano Lett.* **2014**, *14*, 6964–6970.
- (8) Doganov, R. A.; O'Farrell, E. C.; Koenig, S. P.; Yeo, Y.; Ziletti, A.; Carvalho, A.; Campbell, D. K.; Coker, D. F.; Watanabe, K.; Taniguchi, T. Transport properties of pristine few-layer black phosphorus by van der Waals passivation in an inert atmosphere. *Nat. Commun.* **2015**, *6*, 6647.
- (9) Avsar, A.; Vera-Marun, I. J.; Tan, J. Y.; Watanabe, K.; Taniguchi, T.; Castro Neto, A. H.; Özyilmaz, B. Air-Stable Transport in Graphene-Contacted, Fully Encapsulated Ultrathin Black Phosphorus-Based Field-Effect Transistors. *ACS Nano* **2015**, *9*, 4138–4145.
- (10) Perello, D. J.; Chae, S. H.; Song, S.; Lee, Y. H. High-performance n-type black phosphorus transistors with type control via thickness and contact-metal engineering. *Nat. Commun.* **2015**, *6*, 7809.
- (11) Akahama, Y.; Endo, S.; Narita, S.-i. Electrical properties of black phosphorus single crystals. *J. Phys. Soc. Jpn.* **1983**, *52*, 2148–2155.
- (12) Xiang, D.; Han, C.; Wu, J.; Zhong, S.; Liu, Y.; Lin, J.; Zhang, X.-A.; Hu, W. P.; Özyilmaz, B.; Neto, A. C. Surface transfer doping induced effective modulation on ambipolar characteristics of few-layer black phosphorus. *Nat. Commun.* **2015**, *6*, 6485.
- (13) Ho, P. H.; Li, S. S.; Liou, Y. T.; Wen, C. Y.; Chung, Y. H.; Chen, C. W. Wavelength-Selective Dual p-and n-Type Carrier Transport of an Organic/Graphene/Inorganic Heterostructure. *Adv. Mater.* **2015**, *27*, 282–287.
- (14) Konstantatos, G.; Badioli, M.; Gaudreau, L.; Osmond, J.; Bernechea, M.; de Arquer, F. P. G.; Gatti, F.; Koppens, F. H. Hybrid graphene-quantum dot phototransistors with ultrahigh gain. *Nat. Nanotechnol.* **2012**, *7*, 363–368.
- (15) Yu, S. H.; Lee, Y.; Jang, S. K.; Kang, J.; Jeon, J.; Lee, C.; Lee, J. Y.; Kim, H.; Hwang, E.; Lee, S.; Cho, J. H. Dye-Sensitized MoS₂ Photodetector with Enhanced Spectral Photoresponse. *ACS Nano* **2014**, *8*, 8285–8291.
- (16) Kufer, D.; Nikitskiy, I.; Lasanta, T.; Navickaite, G.; Koppens, F. H.; Konstantatos, G. Hybrid 2D–0D MoS₂–PbS Quantum Dot Photodetectors. *Adv. Mater.* **2015**, *27*, 176–180.
- (17) Ho, P.-H.; Yeh, Y.-C.; Wang, D.-Y.; Li, S.-S.; Chen, H.-A.; Chung, Y.-H.; Lin, C.-C.; Wang, W.-H.; Chen, C.-W. Self-encapsulated doping of n-type graphene transistors with extended air stability. *ACS Nano* **2012**, *6*, 6215–6221.
- (18) Cho, S.; Lee, K.; Heeger, A. J. Extended Lifetime of Organic Field-Effect Transistors Encapsulated with Titanium Sub-Oxide as an 'Active' Passivation/Barrier Layer. *Adv. Mater.* **2009**, *21*, 1941–1944.
- (19) Kim, J. Y.; Kim, S. H.; Lee, H.-H.; Lee, K.; Ma, W.; Gong, X.; Heeger, A. J. New architecture for high-efficiency polymer photovoltaic cells using solution-based titanium oxide as an optical spacer. *Adv. Mater.* **2006**, *18*, 572–576.
- (20) Yeh, Y.-C.; Li, S.-S.; Wu, C.-C.; Shao, T.-W.; Kuo, P.-C.; Chen, C.-W. Stoichiometric dependence of TiO_x as a cathode modifier on band alignment of polymer solar cells. *Sol. Energy Mater. Sol. Cells* **2014**, *125*, 233–238.
- (21) Cho, S.; Seo, J. H.; Lee, K.; Heeger, A. J. Enhanced Performance of Fullerene n-Channel Field-Effect Transistors with Titanium Sub-Oxide Injection Layer. *Adv. Funct. Mater.* **2009**, *19*, 1459–1464.
- (22) Lim, J.-H.; Kim, K.-K.; Hwang, D.-K.; Kim, H.-S.; Oh, J.-Y.; Park, S.-J. Formation and effect of thermal annealing for low-resistance Ni/Au ohmic contact to phosphorous-doped p-type ZnO. *J. Electrochem. Soc.* **2005**, *152*, G179–G181.
- (23) Kim, H.-K.; Han, S.-H.; Seonga, T.-Y.; Choi, W.-K. Low-resistance TiO_x/Au ohmic contacts to Al-doped ZnO layers. *Appl. Phys. Lett.* **2000**, *77*, 164710.1063/1.1308527.
- (24) Cai, Y.; Zhang, G.; Zhang, Y.-W. Layer-dependent Band Alignment and Work Function of Few-Layer Phosphorene. *Sci. Rep.* **2014**, *4*, 6677.
- (25) Li, H.-M.; Lee, D.-Y.; Choi, M. S.; Qu, D.; Liu, X.; Ra, C.-H.; Yoo, W. J. Metal-Semiconductor Barrier Modulation for High Photoresponse in Transition Metal Dichalcogenide Field Effect Transistors. *Sci. Rep.* **2014**, *4*, 4041.
- (26) Ho, P.-H.; Lee, W.-C.; Liou, Y.-T.; Chiu, Y.-P.; Shih, Y.-S.; Chen, C.-C.; Su, P.-Y.; Li, M.-K.; Chen, H.-L.; Liang, C.-T. Sunlight-activated graphene-heterostructure transparent cathodes: enabling high-performance n-graphene/p-Si Schottky junction photovoltaics. *Energy Environ. Sci.* **2015**, *8*, 2085–2092.
- (27) Chen, J.-H.; Jang, C.; Adam, S.; Fuhrer, M.; Williams, E.; Ishigami, M. Charged-impurity scattering in graphene. *Nat. Phys.* **2008**, *4*, 377–381.
- (28) Ju, L.; Velasco, J., Jr; Huang, E.; Kahn, S.; Nosiglia, C.; Tsai, H.-Z.; Yang, W.; Taniguchi, T.; Watanabe, K.; Zhang, Y.; Zhang, G.; Crommie, M.; Zettl, A.; Wang, F. Photoinduced doping in heterostructures of graphene and boron nitride. *Nat. Nanotechnol.* **2014**, *9*, 348–352.
- (29) Mimura, T.; Hiyamizu, S.; Fujii, T.; Nanbu, K. A new field-effect transistor with selectively doped GaAs/n-AlxGa1-xAs heterojunctions. *Jpn. J. Appl. Phys.* **1980**, *19*, L225.